Destruction of oxytetracycline using a microwave-assisted fused TiO$_2$ photocatalytic oxidation system

Jaegu Park[*,‡], **Young-Kwon Park**[**,‡], **and Sang-Chul Jung**[*,†]

*Department of Environmental Engineering, Sunchon National University, Sunchon 57922, Korea
**School of Environmental Engineering, University of Seoul, Seoul 02504, Korea

Abstract−We developed a novel and efficient degradation process for oxytetracycline (OTC), an antibiotic that remains in the aquatic environment and affects humans and animals. OTC was decomposed by applying a fusion TiO$_2$ photocatalytic oxidation process adding microwaves, and various unit technologies and their fusion effects were investigated. As the microwave power increased, the decomposition efficiency increased, and the highest decomposition rate was shown in the neutral pH reaction solution. The decomposition rate was greatly increased by the addition of hydrogen peroxide, and it showed a synergistic effect that the decomposition efficiency was doubled by fusion with other processes. Eleven intermediate products of OCT decomposition were detected by liquid chromatography0mass spectrometry; CO$_2$, H$_2$O, NH$_4^+$, and NO$_3^-$ by active oxidizing species, such as OH radicals generated by the microwave-assisted fused TiO$_2$ photocatalytic oxidation process were mineralized.

Keywords: TiO$_2$, Oxytetracycline, Microwave, Electrodeless Lamp, Active Species

INTRODUCTION

Approximately 200,000 tons of antibiotics are manufactured worldwide every year. Among them, tetracycline (TC) is the most common broad-spectrum antibiotic that has been used for bacterial treatments in humans and animals [1,2]. Oxytetracycline (OTC) causes gastrointestinal allergy and photosensitivity allergy, damages calcium-rich areas such as teeth and bones, and candidiasis (thrush) appears to a small extent when used extensively. It is the most widely used tetracycline antibiotic, and it has been detected at ppb to ppm concentrations in water, soil, and food [3]. OTC was observed at concentrations of 46.91 mg L^{-1} in surface water in Austria and 425.1 ng L^{-1} in leachate in Shanghai, China [4]. Several studies have shown that OTC remaining in the environment adversely affects the activities of natural organisms and can cause damage to human life and health [5,6]. Since OTC is chemically stable and has high persistence, it is difficult to effectively remove it, so studies on adsorption methods using various carbon materials and oxidation treatment using photocatalysts are in progress [7-9]. Among them, the oxidation treatment system using a photocatalyst does not generate secondary waste, which is known as an eco-friendly and economical water treatment system [10-12]. However, the water treatment method using the TiO$_2$ photocatalyst has several disadvantages, so it cannot be applied to various water treatments [13]. TiO$_2$ photocatalyst in powder form is difficult to apply to water treatment because it is easily aggregated in water and is not easily recovered after use. In addition, it is difficult to use for efficiently de-grading antibiotics like OTC having a polyaromatic ring structure because of its low degradation rate and lack of reaction selectivity [14].

Our research group made the following attempts to solve the problems of the photocatalytic system. A TiO$_2$ photocatalyst ball to which a TiO$_2$ film is fixed was prepared and used by coating a TiO$_2$ thin film on an alumina ball by chemical vapor deposition (CVD). To utilize strong ultraviolet rays, an electrodeless mercury lamp (EML) emitting light by microwaves was used [15,16]. The use of EML for photocatalytic processes can save money because the lamp is permanently used, and because the amount of light can be freely controlled, the process can be managed efficiently. Hydrogen peroxide was also added to improve the degradation efficiency. In addition, the synergistic effect of each unit process and fusion process was reviewed to assess the possibility of constructing an efficient decomposition system for OTC. This study is a new type of fusion process that compensates for the shortcomings of the existing photocatalytic process, and it is a challenge to draw synergy effects by properly merging various new single processes. The new photocatalytic process developed in this study can effectively decompose OTC, which is difficult to remove with conventional treatment methods, so it is expected that it can be applied to the purification of sewage treatment plants and various drinking water.

EXPERIMENTAL

1. Experimental Materials

Oxytetracycline hydrochloride (C$_{22}$H$_{24}$N$_2$O$_9$·HCl) was purchased from Tokyo Chemical Industry Co. and used as received. The effect of pH on the degradation reaction was examined by adjusting the pH by adding HCl (0.1 N, Daejung Chemical & Metal com.) and NaOH (0.1 N, Daejung Chemical & Metal com.) to the reactant
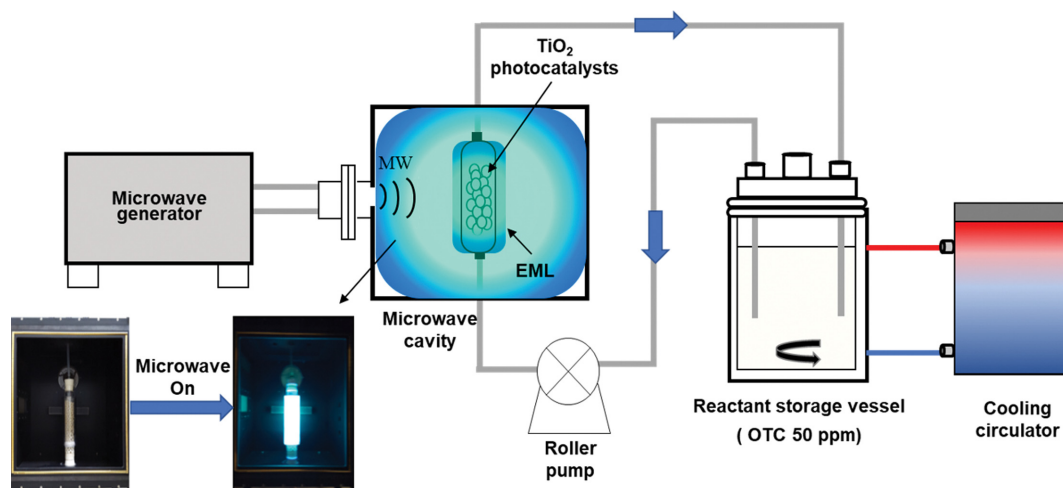
Fig. 1. Schematic diagram of the microwave-assisted fused TiO₂ photocatalytic oxidation system for the OTC decomposition reaction.

solution. The oxidation power in the decomposition reaction was improved by adding a hydrogen peroxide solution (30%, Daejung Chemical & Metal com.) to the aqueous reactant solution. Deionized water was used to prepare the reaction solution, and distilled water was used for the other washings.

2. Experimental Devices

Fig. 1 shows a schematic diagram of the microwave-assisted fused TiO₂ photocatalytic oxidation system used in the OTC decomposition experiment. The frequency of the microwave generator controlled by a power monitor and a three-stub tuner was 2.45 GHz, and maximum power was 1 kW (Korea Microwave Instrument Co., KMIC-1KW). The decomposition experiment was performed while the microwave intensity was changed from 0.2 to 0.8 kW. The microwave emitted to the microwave cavity through the wave-guide emitted EML to supply light to the quartz reactor (length 230 mm, width 40 mm) filled with photocatalytic balls. Fig. 1 (upper left) shows a photograph of the EML emitting microwaves. The spectrum and intensity of light emitted from the EML were measured by optical emission spectroscopy (OES, AVASPEC-2048, Avantes Co. Ltd) and a UV radiometer (Delta OHM, HD2102-2) in the port of the microwave cavity. The temperature was kept constant at 15 °C using a cooling circulator to prevent the temperature of the OCT reaction solution from increasing continuously by microwave radiation and EML emission during the decomposition reaction experiment.

The EML emitting microwaves to the photocatalyst was a double tube type made of quartz. The specifications of the EML are 44 mm in inner diameter, 60 mm in outer diameter, and 170 mm in length. EML produced without a metal electrode because it emits microwave light was made at 10 Torr vacuum by adding a small amount of mercury.

3. OTC Degradation Kinetics Evaluation.

An OTC reaction solution (1,000 mL) with an initial concentration of 50 ppm was prepared, placed in a stainless steel constant temperature storage vessel, and circulated to the photocatalytic reactor. The reaction solution was circulated between the photocatalytic reactor and the reactant storage vessel at 500 mL/min using a roller pump. The reaction solution was circulated through the TiO₂ pho-

tocatalytic system for 10 minutes with the microwave turned off so that the decomposition reaction occurred constantly. H₂O₂ was added to the reaction solution at a concentration of 1 to 100 mM to accelerate the rate of OTC decomposition. The decomposition rate of OTC was determined by measuring the concentration of OTC in the reaction solution sample as a function of reaction time. The OTC concentration in the sample was measured at 353 nm, the maximum absorption wavelength of OTC, by a UV-vis spectrophotometer (Shimadzu, UV-1280).

The intermediate-products generated during OTC degradation by microwave-assisted fused TiO₂ photocatalytic oxidation were detected using triple quadrupole liquid chromatography-tandem mass spectrometry (Shimadzu LCMS-8060NX). The column used was ZORBAX Eclipse XDB-C18 (inner diameter 2.1 mm×length 50 mm), and the injection volume was 10 μL. The mobile phase A was 0.1% formic acid aqueous solution, and mobile phase B was a 0.1% formic acid–acetonitrile solution. The flow rate was maintained at 0.3 mL/min. In positive ESI mode, the intermediates were estimated from the m/z values of the substances produced in the OTC decomposition reaction.

RESULTS AND DISCUSSION

1. Characteristics of the Light Source Emitted by the EML

The EML used in this study was a lamp that does not use a metal electrode because it emits light by microwaves and emits light by the mercury charged inside the lamp in a low vacuum state. The TiO₂ photocatalyst can be excited by ultraviolet rays. Although the EML irradiates a wide range of light in the ultraviolet and visible regions, the light sources in the ultraviolet region were reviewed based on the photocatalytic properties of TiO₂. The spectrum of the emitted ultraviolet region was measured by OES to evaluate the ultraviolet emission characteristics of the EML, as shown in Fig. 2. In the UV-C region, strong light by atomic Hg (6^2P_1-6^2S_0) was emitted at 253.7 nm, and light was emitted at 297 nm and 313 nm in the UV-B region [17]. In addition, ultraviolet rays at 365 nm were emitted in the UV-A region.
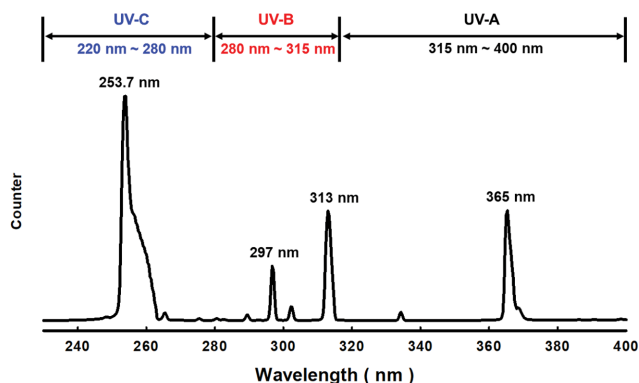
Fig. 2. Optical emission spectroscopy spectra of the EML.

The effect of microwave power on the amount of UV emission of EML was investigated. Fig. 4 shows the change in the amount of ultraviolet light emitted from the EML according to the change in microwave intensity. The change in the quantity of photons emitted at 365, 297, and 254 nm according to the change in microwave intensity was measured by OES (Fig. 3(a)). The quantity of photons emitted at 254 nm, which is the UV-C region, was the largest, with the quantity of photons emitted at 297 nm being the lowest. The photons emitted at 254 nm, which is UV-C, increased gradually with increasing microwave intensity. On the other hand, photons emitted at 297 and 365 nm, which are UV-B and UV-A, increased rapidly with increasing microwave intensity up to 0.5 kW, and then increased gradually above that. The intensity of the ultraviolet rays emitted from the EML for each ultraviolet region (UV-A, UV-B, and UV-C) was measured using a UV radiometer (Fig. 3(b)). The UV radiometer sensor was attached in the external port of the microwave cavity 30 cm away from the EML. The range of UV wavelengths detected by each sensor during the intensity measurements was UV-A 315-400 nm, UV-B 280-315 nm, and UV-C 220-280 nm. Most of the ultraviolet rays generated from the EML were
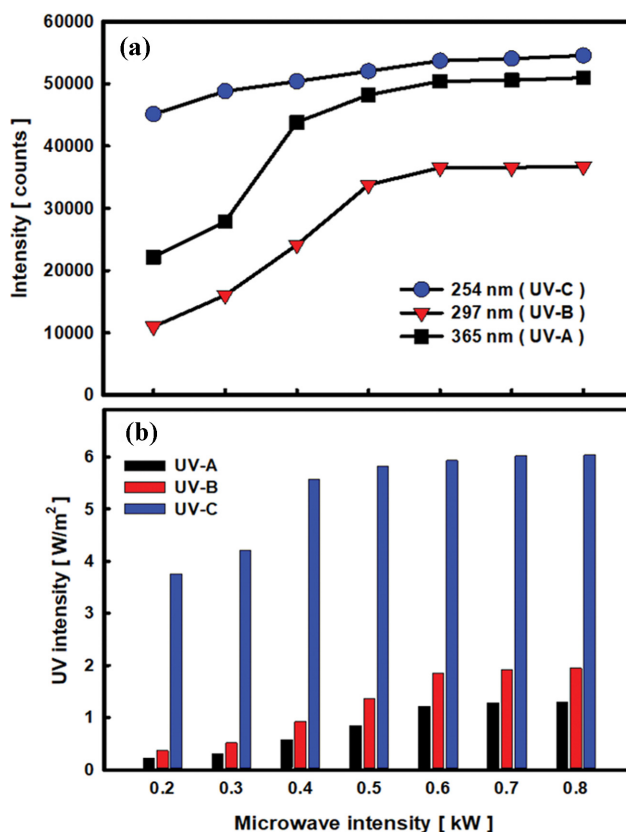

Fig. 3. Changes in the amount of ultraviolet light emitted from the EML according to microwave intensity changes.

high-energy short-wave ultraviolet rays corresponding to UV-C. Light with a shorter wavelength has higher energy. In particular, the UV-C region has a high-energy value of 6.2 eV, showing the highest intensity [18]. With the same result as in Fig. 3(a), the intensity increased rapidly when the microwave output was low, and then
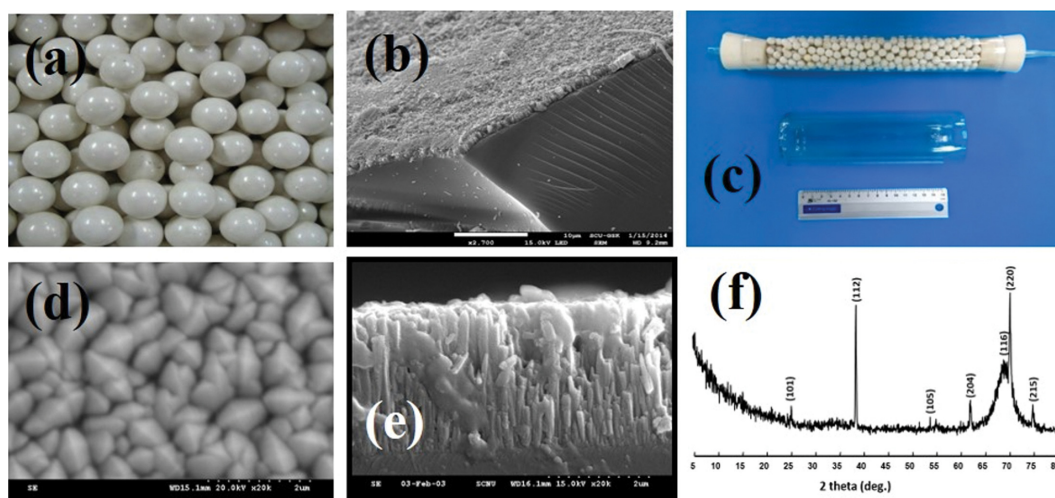

Fig. 4. Images of TiO₂ photocatalyst balls prepared by CVD. (a) real photo-image of TiO₂ photocatalyst balls, (b) SEM image of a TiO₂ photocatalyst ball, (c) photo-image of photolysis reactor and EML, (d) SEM image of the TiO₂ film surface, (e) SEM image of a cross-section of the TiO₂ film, (f) X-ray diffraction pattern of the TiO₂ film.
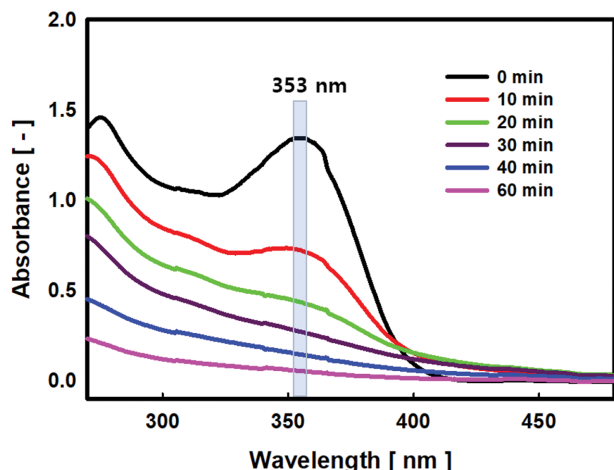
Fig. 5. Change in absorbance according to reaction time in OTC decomposition reaction by TiO₂ photocatalytic process using the EML.

Fig. 6. Effect of microwave power on the OTC decomposition reaction by TiO₂ photocatalytic process using EML.

Fig. 7. Effect of pH of the OTC reaction solution on the OTC decomposition reaction rate.

gradually increased over 0.5 kW.

2. Evaluation of the OTC Degradation Rate

A photocatalyst ball coated on an alumina ball (ø 8 mm) by CVD was used for the decomposition experiment, as shown in Figs. 4(a) and (b). Fig. 4(c) shows the reactor (40 mm diameter, 230 mm length) made of quartz filled with photocatalyst balls. Fig. 4(d) and (e) show SEM images of the surface and cross-section of the coated TiO₂ film. The coated TiO₂ film was anatase crystals oriented on the 112 and 220 planes, and the XRD pattern was shown in Fig. 4(f). Details of the preparation method and process conditions of the CVD TiO₂ film have been described [19,20].

In this study, the OTC decomposition reaction rate was calculated from the absorbance measured in the spectrophotometer. Fig. 5 presents the change in the absorbance of OTC according to the reaction time by the TiO₂ photocatalyst system using the lamp emitted by microwave. At this time, microwave discharge power was performed at 0.6 kW. The absorbance at the maximum wavelength of 353 nm decreased with increasing decomposition reaction time. This confirmed that OTC had decomposed by the TiO₂ photocatalytic process using an EML.

Fig. 6 shows the effect of the microwave power on the decomposition rate in the OTC decomposition reaction by the TiO₂ photocatalytic process using an EML. The decomposition rate of OTC increased with increasing microwave power, and showed a reaction rate constant of 6.16×10^{-2} min^{-1} at the maximum power of 0.8 kW. On the other hand, although a large increase in the decomposition rate was shown in the section with low microwave power, the reaction rate was similar at 0.6 kW and 0.8 kW. Fig. 4 shows the change in ultraviolet rays emitted from the EML according to the change in microwave intensity. The change in the intensity of ultraviolet rays was small above 0.5 kW. Correspondingly, it was assumed that the difference in decomposition rates at 0.6 kW and 0.8 kW was small. These results show that the TiO₂ photocatalytic decomposition process using an EML was greatly affected by the emitted ultraviolet light.

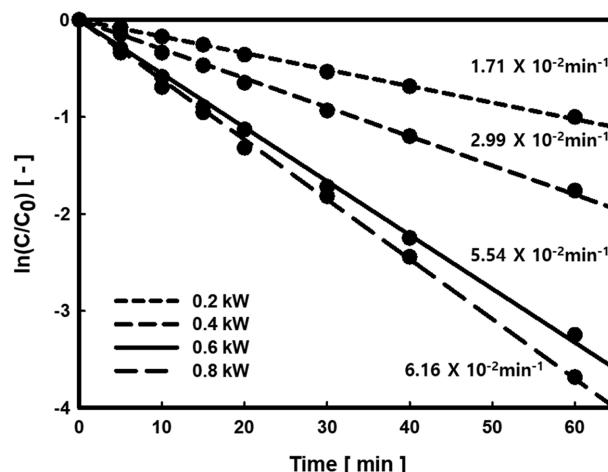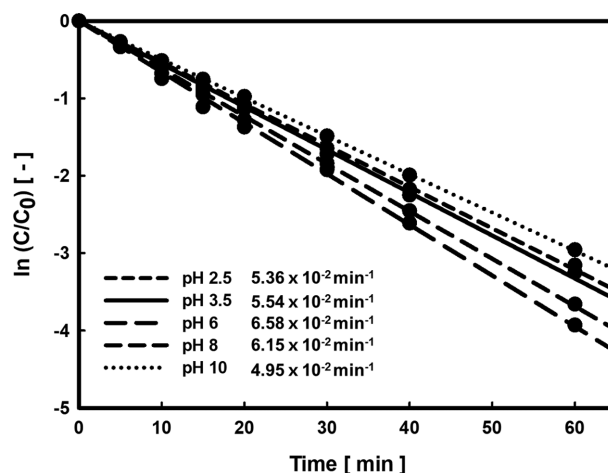pH is a major factor influencing the operation of OTC and the

environment, such as oxygen presence and flow [20]. The effects of the pH of the reaction solution on the decomposition reaction of OTC using the TiO₂ photocatalytic process applied with an EML were investigated. In this study, the OTC decomposition reaction rate was evaluated by adjusting the pH of the OTC reaction solution to 2.5-10 using 0.1 N NaOH and 0.1 N HCl. The effects of the pH of the OTC reaction solution on the decomposition reaction are shown as the change according to the reaction time and the change in the rate constant (Fig. 7). At pH 2.5 with HCl added to the reaction aqueous solution, the decomposition rate was reduced compared to the OCT reaction solution to which nothing had been added. Although the highest decomposition rate was observed at pH 6 in which NaOH had been added to the aqueous reaction solution, the decomposition rate decreased under basic conditions. OTC is a molecule with several functional groups capable of ionization in different pH ranges [22]. When the OTC reaction solution has a pH of 2, OTC is protonated to H_3OTC^+. At pH 8.5, OTC is present in the reaction solution mainly as $HOTC^-$, and at pH 11 it exists as OTC^{2-} [23]. On the other hand, OTC exists as a

zwitterion with a positive charge due to a tertiary amine functional group in the pH range of 4-8 and a negative charge on the deprotonated hydroxyl group [24]. The decrease in the decomposition rate under acidic and basic conditions can be explained by considering the properties of the TiO$_2$ photocatalyst and OTC. TiO$_2$ has an uncharged zero point charge (ZPC) of approximately 6.7 on the surface. Accordingly, TiO$_2$ has a positive charge at pH<6.7, and a negative charge at pH>6.7. In an OTC reaction solution with a pH=6, OTC is mostly present as a zwitterion with a small amount of HOTC$^-$. Therefore, it has high decomposition efficiency under neutral conditions, where the electrostatic attraction with the positively charged TiO$_2$ surface is increased [23]. In an acidic aqueous reaction solution, TiO$_2$ has a positive charge, and OTC exists as HOTC$^+$, so both materials have a positive charge. Therefore, the decomposition rate is reduced by electrostatic repulsion. When the reaction solution is basic, TiO$_2$ is negatively charged, and OTC is also negatively charged as OTC^{2-}. Hence, the decomposition rate is also reduced due to electrostatic repulsion [19].

Hydrogen peroxide was added to the reaction solution to increase the OTC decomposition rate. Hydrogen peroxide was adjusted to 1-100 mM. The microwave power was 0.6 kW and the pH of the reaction solution was 3.5. Fig. 8 shows the results of the OTC decomposition reaction rate according to the change in hydrogen peroxide concentration. The rate of OTC decomposition increased with increasing concentration of H$_2$O$_2$ added, and even when only 1 mM was added, the decomposition efficiency doubled, showing a reaction rate constant of 10.87×10^{-2} min^{-1}. The degradation rate constant k of the reaction solution, in which hydrogen peroxide was added at 10 mM and 100 mM, was very high at 32.03×10^{-2} min^{-1} and 39.28×10^{-2} min^{-1}, respectively. When hydrogen peroxide was injected into the reaction solution, electrons emitted from TiO$_2$ decreased and the generation of hydroxyl radicals increased through reaction with superoxide anion radicals. Strong chemically active species, such as hydroxyl anion and oxygen gas, were generated [24]. Therefore, the number of hydroxyl radicals formed in the TiO$_2$ photocatalyst was increased by the addition of H$_2$O$_2$, and thus the decomposition efficiency of OTC was improved.
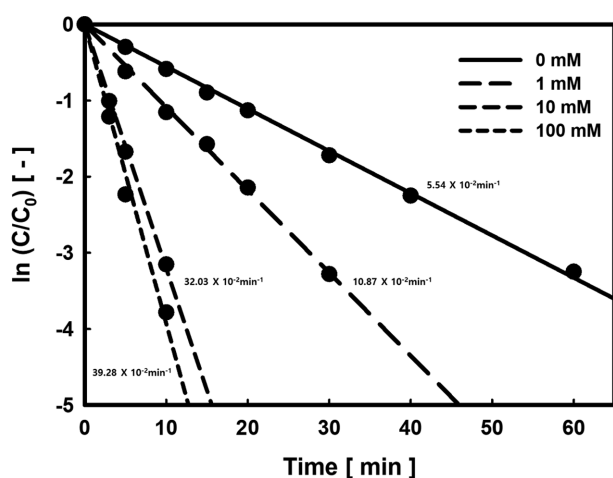

Fig. 8. Effect of hydrogen peroxide addition on the OTC decomposition reaction rate.
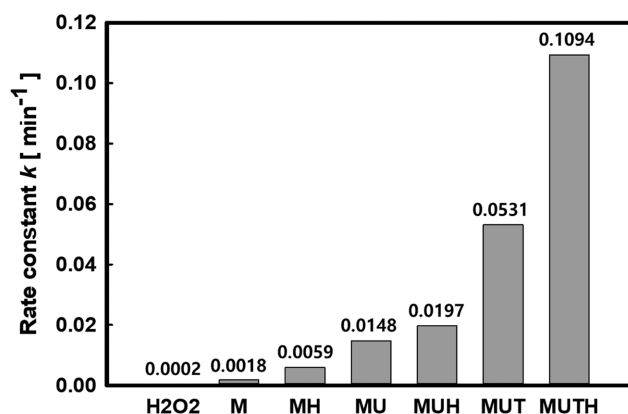

Fig. 9. Degradation reaction rate constants of OTC obtained under different experimental conditions.

This study reviewed the effects of each unit technology and complex processes in the OTC decomposition reaction using the microwave-assisted fused TiO$_2$ photocatalytic oxidation system. Fig. 9 presents the reaction rate constants obtained from the OTC decomposition reaction by the element technologies and the fusion processes that combine them. In this experiment, a microwave discharge power of 0.6 kW, pH of 3.5, and hydrogen peroxide 1 mM were added. H in Fig. 9 is a reaction in which hydrogen peroxide is simply added to the OTC reaction solution; OTC was hardly decomposed. It was not decomposed by an oxidizing agent, such as hydrogen peroxide, and had a strong binding force [25]. M is a reaction in which only the OTC reaction solution is irradiated with microwaves; again, OTC barely decomposed. MH is a reaction in which an aqueous OTC reaction solution containing hydrogen peroxide is irradiated with microwaves. OTC was decomposed at a low decomposition rate. Hydrogen peroxide alone could not decompose OTC, but OTC could be decomposed with the aid of microwaves. MU is an OTC decomposition reaction by the EML emitting microwaves and exhibited a decomposition reaction rate constant of 1.48×10^{-2} min^{-1}. The bond of OTC was broken by light energy, such as ultraviolet rays emitted from the EML. MUH is an OTC reaction solution containing hydrogen peroxide that was exposed to the EML emitting microwave and exhibited a decomposition reaction rate constant of 1.97×10^{-2} min^{-1}. The MUT used a TiO$_2$ photocatalyst and EML emitting microwave and exhibited a decomposition reaction rate constant of 5.31×10^{-2} min^{-1}. The decomposition rate of OTC by MUT was judged to be high, and the performance of the CVD TiO$_2$ photocatalyst balls applied in this study was excellent. MUTH is an OTC decomposition reaction in which H$_2$O$_2$ is added to the MUT reaction, and exhibited a decomposition rate constant of 1.09×10^{-1} min^{-1}. The rate of OTC decomposition by MUTH was very high, and approximately 95% of OTC was removed within 60 minutes. On the other hand, MUTH showed approximately double the decomposition reaction of MUT, and it was presumed that the use of the TiO$_2$ photocatalyst and hydrogen peroxide as an oxidizing agent has a synergistic effect on OTC decomposition.

3. Suggested Pathway for Degradation of OTC

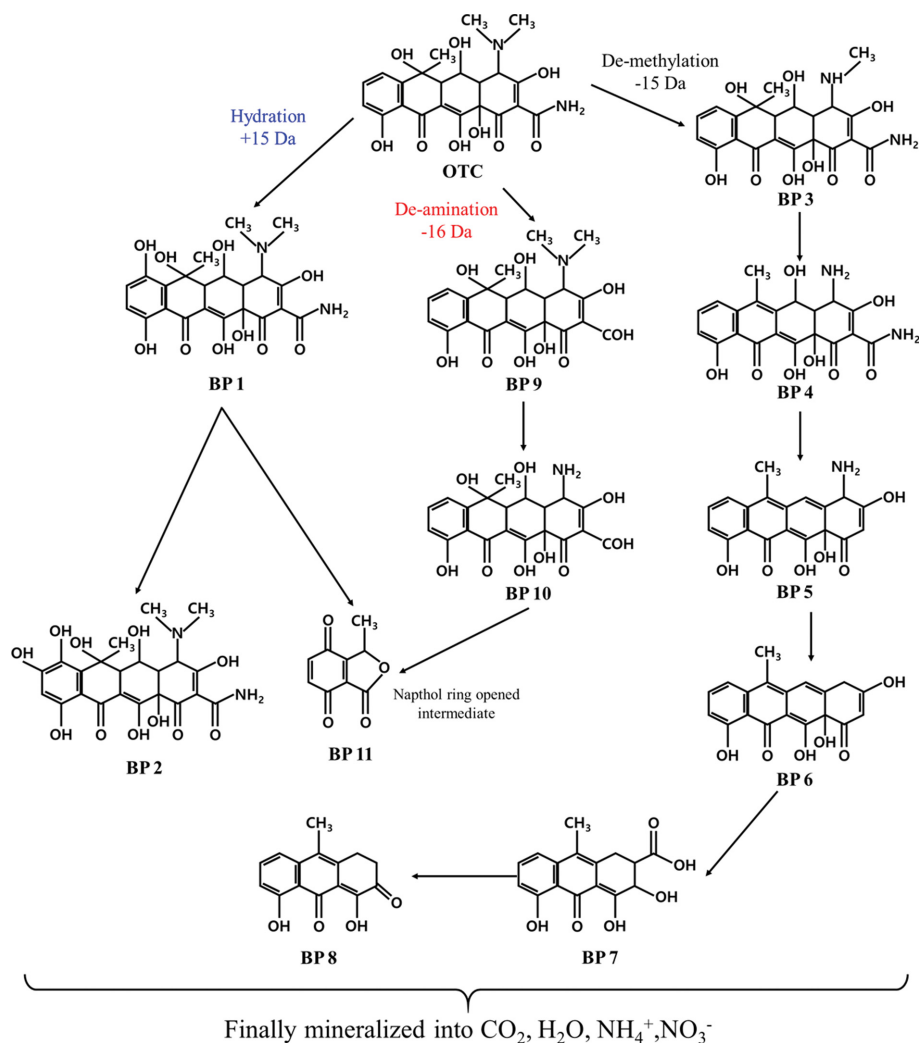In the OTC decomposition reaction using a microwave-assisted

Fig. 10. Proposed degradation pathway of oxytetracycline using the microwave-assisted fused TiO₂ photocatalytic oxidation system.

fused TiO_2 photocatalytic oxidation system, intermediates generated during the reaction were detected by LCMS to trace the decomposition reaction mechanism. In this experiment, a microwave intensity of 0.6 kW, pH 3.5, and hydrogen peroxide concentration of 1 mM were used. Eleven different intermediates were detected by LC-MS. Table 1 lists the molecular weight, formula, and possible chemical structure of the intermediates detected by LC-MS analysis.

The predictable decomposition pathway of the OTC decomposition reaction using the microwave-assisted fused TiO_2 photocatalytic oxidation process is shown in Fig. 10. OTC degradation performed in this study was estimated to be caused by reactions, such as hydration, dehydration, demethylation, de-hydroxylation, and ring cleavage. Powerful oxidizing hydroxyl radicals generated by the microwave-assisted fused TiO_2 photocatalytic oxidation process, can affect the aromatic ring of OTC, which is likely to generate m/z 476 (BP 1) and m/z 492 (BP 2) through the hydroxyl reaction [26]. The naphthol ring of BP 1 can generate m/z 178 (BP 11) through hydroxyl radical attack [27]. On the other hand, OTC is removed from the N-methyl group by demethylation induced in

the photooxidation reaction, and m/z 446 (BP 3) can be produced [28]. BP 3 can be decomposed to m/z 414 (BP 4) by removing the N-methyl and hydroxyl groups by demethylation and de-hydroxylation, respectively. BP 4 can be decomposed further to m/z 371 through de-carboxamidation, and m/z 353 (BP 5) can then be generated through the dehydration path. BP 5 can be decomposed to m/z 338 (BP 6) through de-amination. Hydroxyl radicals and superoxide anion radicals, which are strongly oxidative active species generated in the microwave-assisted fused TiO_2 photocatalytic oxidation process, attack the double bond of BP 6 and can be decomposed to m/z 302 (BP 7) through ring cleavage. BP 7 can be degraded to m/z 256 (BP 8) through de-carboxylation and dehydration, and to m/z 445 (BP 9) through de-amination [26]. BP 9 can be decomposed to m/z 401 (BP 10) because of the loss of two N-methyl groups in the aromatic ring by attack by oxidizing species because of the low binding energy of N-C. BP10 can be decomposed to BP11 by opening the naphthol ring by hydroxyl radicals [23]. OTC will be decomposed through the above pathways, and the intermediates produced are expected to be decomposed to low molecular weight organic compounds through an additional reac-

Table 1. Intermediate product of OTC decomposed by microwave-assisted fused TiO₂ photocatalytic oxidation process

No.	Molecular weight (m/z)	Formula	Possible chemical structure
OTC	461	$C_{22}H_{24}N_2O_9$	
BP 1	476	$C_{22}H_{24}N_2O_{10}$	
BP 2	492	$C_{22}H_{24}N_2O_{11}$	
BP 3	446	$C_{21}H_{22}N_2O_9$	
BP 4	414	$C_{20}H_{18}N_2O_8$	
BP 5	353	$C_{19}H_{15}NO_6$	
BP 6	338	$C_{19}H_{14}O_6$	
BP 7	302	$C_{16}H_{14}O_6$	
BP 8	256	$C_{15}H_{12}O_4$	
BP 9	445	$C_{22}H_{23}NO_9$	
BP 10	401	$C_{20}H_{19}NO_8$	
BP 11	178	$C_9H_6O_4$	

tion. Finally, OTC is expected to be mineralized to end products, such as CO_2, H_2O, NH_4^+, and NO_3^- [26-29].

CONCLUSIONS

OTC was decomposed using a novel microwave-assisted fused TiO₂ photocatalytic oxidation process, with CVD TiO₂ photocatalytic balls and EML as light sources. As the microwave power increased, the amount of UV light emitted from the EML increased, but there was no further increase at 0.5 kW or more. As the microwave power increased, the decomposition rate of OTC increased, and the reaction solution at pH 6 showed the highest decomposition efficiency. The decomposition reaction did not occur when only H_2O_2 was added to the OTC reaction solution, but the reaction efficiency was increased rapidly when combined with other elemental technologies. Although OTC was decomposed only with light energy irradiated from microwaves and the EML, the decomposition efficiency was increased significantly when combined with a TiO₂ photocatalyst. In particular, a rapid increase in decomposition efficiency was observed when H_2O_2 was added to the microwave-assisted TiO₂ photocatalytic process. OTC was finally mineralized to CO_2, H_2O, NH_4^+ and NO_3^- by reactions such as hydration, dehydration, demethylation, dehydration oxidation and ring cleavage by active oxidizing species such as OH radicals formed in the microwave assisted fused TiO₂ photocatalytic oxidation process.

ACKNOWLEDGEMENTS

REFERENCE

1. S. Vaz, *Chem. Biol. Technol. Agric.*, **3**, 6 (2016).
2. Q. Liu, H. Yu, F. Zeng, X. Li, J. Sun, X. Hu, Q. Pan, C. Li, H. Lin and Z. M. Su, *J. Colloid Interface Sci.*, **579**, 119 (2020).
3. X. Ren, Z. Wang, B. Gao, P. Liu and J. Li, *Chemosphere*, **173**, 563 (2017).
4. M. C. Elena, G. B. Carmen, S. Sigrid and G. Oliver, *Environ. Pollut.*, **148**, 570 (2007).
5. J. Rok, D. Wrzésniok, A. Beberok, M. Otręba, M. Delijewski and E. Buszman, *Toxicol. Vitro*, **48**, 26 (2018).
6. A. R. Almeida, I. Domingues and I. Henriques, *Environ. Pollut.*, **272**, 116371 (2021).
7. W. Yan, Y. Guo, Y. Xiao, S. Wang, R. Ding, J. Jiang, H. Gang, H. Wang, J. Yang and F. Zhao, *Water Res.*, **142**, 105 (2018).
8. Y. Zhang, S. U. Geißen and C. Gal, *Chemosphere*, **73**, 1151 (2008).
9. S. Wu, H. Hu, Y. Lin, J. Zhang and Y. H. Hu, *Chem. Eng. J.*, **382**, 122842 (2020).
10. H. Lee, S. H. Park, Y. K. Park, S. J. Kim, S. G. Seo, S. J. Ki and S. C. Jung, *Chem. Eng. J.*, **278**, 259 (2015).
11. H. Lee, Y. K. Park, S. J. Kim, B. H. Kim, H. S. Yoon and S. C. Jung, *J. Ind. Eng. Chem.*, **35**, 205 (2016).
12. S. J. Ki, K. J. Jeon, Y. K. Park, S. Jeong, H. Lee and S. C. Jung, *Catal. Today*, **293**, 15 (2017).
13. S. H. Park, S. J. Kim, S. G. Seo and S. C. Jung, *Nanoscale Res. Lett.*, **5**, 1627 (2010).
14. S. C. Jung, *Water Sci. Technol.*, **63**, 1491 (2011).
15. S. Jeong, H. Lee, H. Park, K. J. Jeon, Y. K. Park and S. C. Jung, *Catal. Today*, **307**, 65 (2018).
16. D. J. Lee, Y. K. Park, S. J. Kim, H. Lee and S. C. Jung, *Korean J. Chem. Eng.*, **32**, 1188 (2015).
17. U. Gross, A. Ubelis, P. Spietz and J. Burrows, *J. Phys. D: Appl. Phys.*, **33**, 1588 (2000).

18. F. Behar-cohen, G. Baillet, J. Krutmann and P. Pena-garcia, *Clin. Ophthalmol.*, **8**, 87 (2013).

19. S. C. Jung, *Korean J. Chem. Eng.*, **25**, 364 (2008).

20. S. J. Kim, S. C. Kim, S. G. Seo, D. J. Lee, H. Lee, S. H. Park and S. C. Jung, *Catal. Today*, **164**, 384 (2011).

21. M. Bennemla, M. Chabani and A. Amrane, *Int. J. Chem. Kinet.*, **48**, 464 (2016).

22. W. Kong, C. Li, J. M. Dolhi, S. Li, J. He and M. Qiao, *Chemosphere*, **87**, 542 (2012).

23. R. Li, Y. Jia, J. Wu and Q. Zhen, *RSC Adv.*, **5**, 40764 (2015).

24. S. C. Jung, H. Lee, S. J. Ki, S. J. Kim and Y. K. Park, *Catal. Today*, **348**, 270 (2020).

25. M. Zouanti, M. Bezzina and R. Dhib, *Environ. Eng. Res.*, **25**, 316 (2020).

26. S. Zhang, S. Zhao, S. Huang, B. Hu, M. Wang, Z. Zhang, L. He and M. Du, *Chem. Eng. J.*, **420**, 130516 (2021).

27. J. Niu, S. Ding, L. Zhang, J. Zhao and C. Feng, *Chemosphere*, **93**, 1 (2013).

28. Y. Liu, X. He, Y. Fu and D. D. Dionysiou, *J. Hazard. Mater.*, **305**, 229 (2016).

29. J. H. O. S. Pereira, V. J. P. Vilar, M. T. Borges, O. González, S. Esplugas and R. A. R. Boaventura, *Sol. Energy*, **85**, 2732 (2011).